

DESIGN OF AN ELECTROSTATIC DEFLECTOR
FOR THE ION BEAM OF THE
OREGON STATE COLLEGE CYCLOTRON

by

HAROLD PATTERSON MAHON, JUNIOR

A THESIS

submitted to

OREGON STATE COLLEGE

in partial fulfillment of
the requirements for the
degree of

MASTER OF SCIENCE

June 1955

APPROVED:

Redacted for Privacy

Professor of Physics

In Charge of Major

Redacted for Privacy

Chairman of Department of Physics

Redacted for Privacy

Chairman of School Graduate Committee

Redacted for Privacy

Dean of Graduate School

Date thesis is presented Aug. 12, 1954

Typed by Ruth Perry

ACKNOWLEDGEMENT

The author wishes to express his gratitude to Dr. R. R. Dempster for his guidance and patience during the preparation of this thesis. The author also wishes to thank D. B. Nicodemus, and E. A. Yunker, of Oregon State College and T. J. Morgan and J. H. Manley of the University of Washington for helpful suggestions and aid in obtaining information for this thesis.

TABLE OF CONTENTS

	<u>Page</u>
Introduction	1
Channel Width Considerations	9
The Deflecting Field	18
Calculation of the Path of the Ion	32
Conclusion	51
Bibliography	57

LIST OF FIGURES

Figure		Page
1	The D. C. Deflector	4
2	The R.F. Deflector	7
3	Diagram Used to Determine Channel Spacing Function	14
4	Sectional View of the Cyclotron from the Air Gap	22
5	Scale Drawing of Vacuum Chamber and Dees	28
6	Graph of the Magnetic Induction in the Region of the Deflector	35
7	Graph of the Magnetic Induction at the Edge of the Cyclotron Magnet	36
8	Construction of the Ion Path $\phi = 150^\circ$, $V_{DC} = 10,000$ volts	41
9	Construction of the Ion Path $\phi = 150^\circ$, $V_{DC} = 0$	44
10	Plot of the Ion Path $\phi = 150^\circ$, $V_{DC} = 20,000$ volts	46
11	Plot of the Ion Path $\phi = 160^\circ$, $V_{DC} = 10,000$ volts	48
12	Plot of the Ion Path $\phi = 170^\circ$, $V_{DC} = 15,000$ volts	49
13	Final Deflector Geometry	50

LIST OF TABLES

Table		Page
1	Channel Spacing	17
2	Approximate Values of the Radius of Curvature of the Ion Path at the Entrance to the Channel	29
3	Values of $8 \times 10^{-4} E$	37
4	Values for the Computations Used in Plotting the Ion Paths	53

DESIGN OF AN ELECTROSTATIC DEFLECTOR
FOR THE ION BEAM OF THE
OREGON STATE COLLEGE CYCLOTRON

INTRODUCTION

Particle accelerators may be either: (1) devices in which the particle receives all of its energy in a single acceleration through a large potential difference, as in the case of the X-ray tube, or (2) devices in which the particle gains its energy in repeated accelerations through a series of small potential differences. The highest energy particles are attained by the second method and the cyclotron is the preeminent machine of this type.

The cyclotron is a prolific source of high energy ions that have found numerous uses in the production of radioisotopes and scientific investigation. The cyclotron was developed by Ernest O. Lawrence (13, pp. 19-35) of the University of California beginning in 1930, who won the Nobel prize in 1939 for his work in this field.

The high velocities of the particles in the cyclotron are attained by accelerations through a relatively small potential a number of times, rather than just once through a high potential. The problem of high voltage insulation therefore is eliminated since the voltages used need not be excessive. Between the poles of a large electromagnet is located a vacuum chamber containing the two semi-circular, flat, hollow electrodes. These electrodes are called dees from their resemblance to the letter D. Positively charged ions are formed in the center of the vacuum chamber between the dees.

When one electrode is positively charged and the other electrode is negatively charged, the ion will be accelerated toward the negative electrode. After the ion passes inside the hollow electrode it is no longer affected by the electric field. However, the ion is always acted upon by the magnetic field which causes it to move in a circular path. After the particle has completed a half circle it is again between the two electrodes. If the half period of the alternating radio frequency potential applied to the dees is the same as the time necessary for the ion to travel this half circle¹, the polarity of the dees will have changed so that the particle is again approaching a negative electrode, and hence is accelerated to a higher velocity. The positive ion path will now have a larger radius as it follows its circular path in the magnetic field. This process will continue. The ion will gain in velocity every time it crosses the gap between the dees, and will spiral outward with an ever-increasing radius of curvature. If the average voltage between the dees is 75,000 volts when the ion crosses the gap 100 times (in 50 revolutions), the ion's velocity will be as if it had fallen through a single potential difference of 7,500,000 volts. The dees are enclosed in a vacuum chamber so that the ion may travel without colliding with other atoms. For deuterons for the polarity of the accelerating voltage to change every time the ion crosses the gap, the accelerating potential must have a frequency of about 10,500,000 cycles per second, at a magnetic induction of 14,000 gauss. Excellent descriptions of the cyclotron have been

¹ The angular frequency of an ion in a constant magnetic field is constant.

given by Fremlin and Gooden (4, pp. 295-348), by Livingston (17, pp. 128-147 and 18, pp. 269-315) and by Mann (20, pp. 125-136, and 21).

To make the maximum use of the intense beam of energetic ions, it may be possible to use an internal target². Since a 7.5 Mev (million electron volt) beam may concentrate as much as 4,000 watts of power on an area only a few millimeters square, internal target materials must be limited to those non-volatile substances possessing a high heat conductivity so that they are capable of being adequately cooled by a water cooled rotating support. There are many problems involved with the use of internal targets because of the high intensity of the beam.

The beam may be brought outside the cyclotron through a thin metal foil window where, due to the natural spreading of the beam, a less intense beam is available. Targets that must be cooled by a stream of inert gas because of their poor heat conductivity may now be irradiated. Liquids and gases, and materials which may spatter or otherwise contaminate the vacuum chamber may be also used as targets with an external beam. An external beam may be used in experiments requiring a linear beam, or the absence of the strong magnetic field in the region of the cyclotron. Twenty to thirty per cent of the positive ions may be deflected from their circular path in the magnetic field onto an external target by means of an electric field perpendicular to the Lorentz magnetic force. This electric field is produced by a mechanism called the "deflector".

² Probe currents of 12 Mev deuterons as large as 1 milliampere have been observed in the MIT cyclotron (17, p. 129).

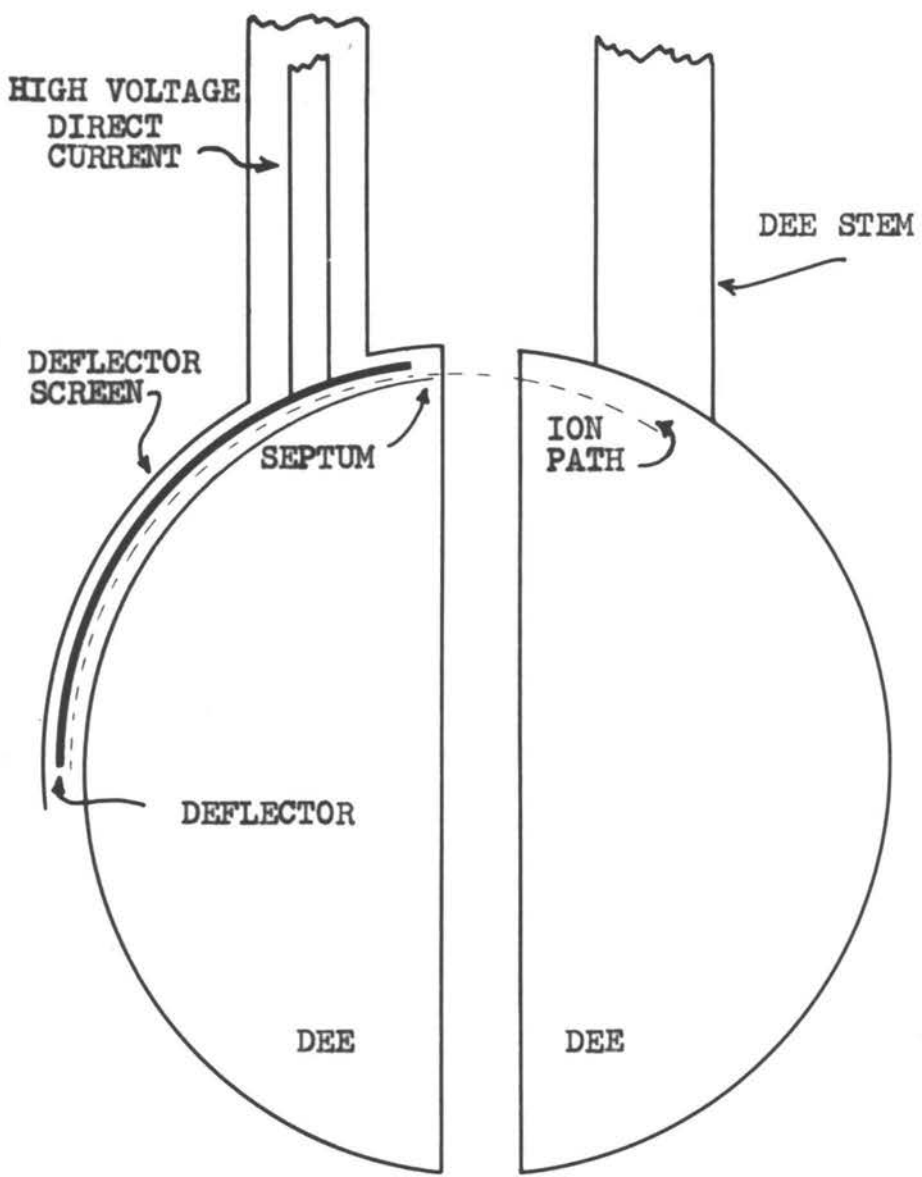


FIGURE 1.
THE D.C. DEFLECTOR SYSTEM

It is the purpose of this thesis to propose a design of an electrostatic deflector for the Oregon State College cyclotron.

There are two general classes of electrostatic deflectors:

(1) devices on which the applied voltage is D.C. (Direct Current) only, and (2) devices on which the deflecting potential is a sum of the instantaneous R.F. (Radio Frequency) voltage on the dee and the constant D.C. voltage applied.

The D.C. deflector, illustrated in Figure 1, allows complete control over the deflecting potential that is independent of the phase of the circulating ions. Also no capacitance is added to the dee system by the deflector. This is important so that a large part of the R.F. power input to the dees will not be lost through the deflector and so that it will not unbalance the tuned circuit of the dee R.F. power supply in systems using a master oscillator where this may be important. Installations where a D.C. deflector was employed have been the first University of California cyclotron described by Lawrence and Livingston (13, pp. 19-35), the MIT cyclotron described by Livingston (17, pp. 128-147), and the Birmingham University cyclotron described by Fremlin and Gooden (4, pp. 307-309).

However, there are many disadvantages with a D.C. deflector. Extremely high potentials are required to pull the ions away from the magnetic field which tends to hold them in a circular path. Because it is necessary to shield the D.C. deflector from the R.F. power supply to the dees, the deflector support must be run through the dee stem. Mechanical adjustment of the deflector, which may be internally

located in one of the dees in some installations, is therefore difficult.

Many recent cyclotron designs are using the R.F. deflector, which eliminates some of the problems associated with the D.C. deflector. The R.F. deflector utilizes the high R.F. potentials existing on the dees to deflect the ion beam. In situations where this potential is insufficient to deflect the beam as desired the difference between the average deflecting field from the dee voltage and the necessary deflecting field, may be supplied by a relatively low D.C. potential.

The R.F. deflector is a strip of metal extending over an arc of 60 to 90 degrees that forms one side of the deflecting channel. The edge of the dee is built out with a strip of metal to form the other side of the deflector channel. (Refer to Figure 2.) The channel is the region through which the ions pass and in which the electrostatic field is formed. At the entrance to the channel there is a strip of metal in the edge of the dee called the septum.

The use of the instantaneous voltage on the dee to produce a deflecting field is possible by connecting the deflector through a large condenser to ground. Adjustment of the deflecting field may be made simply by altering the deflector spacing, and by varying the potential applied to the deflector; this is an important advantage of the R.F. deflector as compared to the D.C. deflector.

Installations not using a self-excited oscillator for the dee power supply may compensate for the capacitance of the deflector,

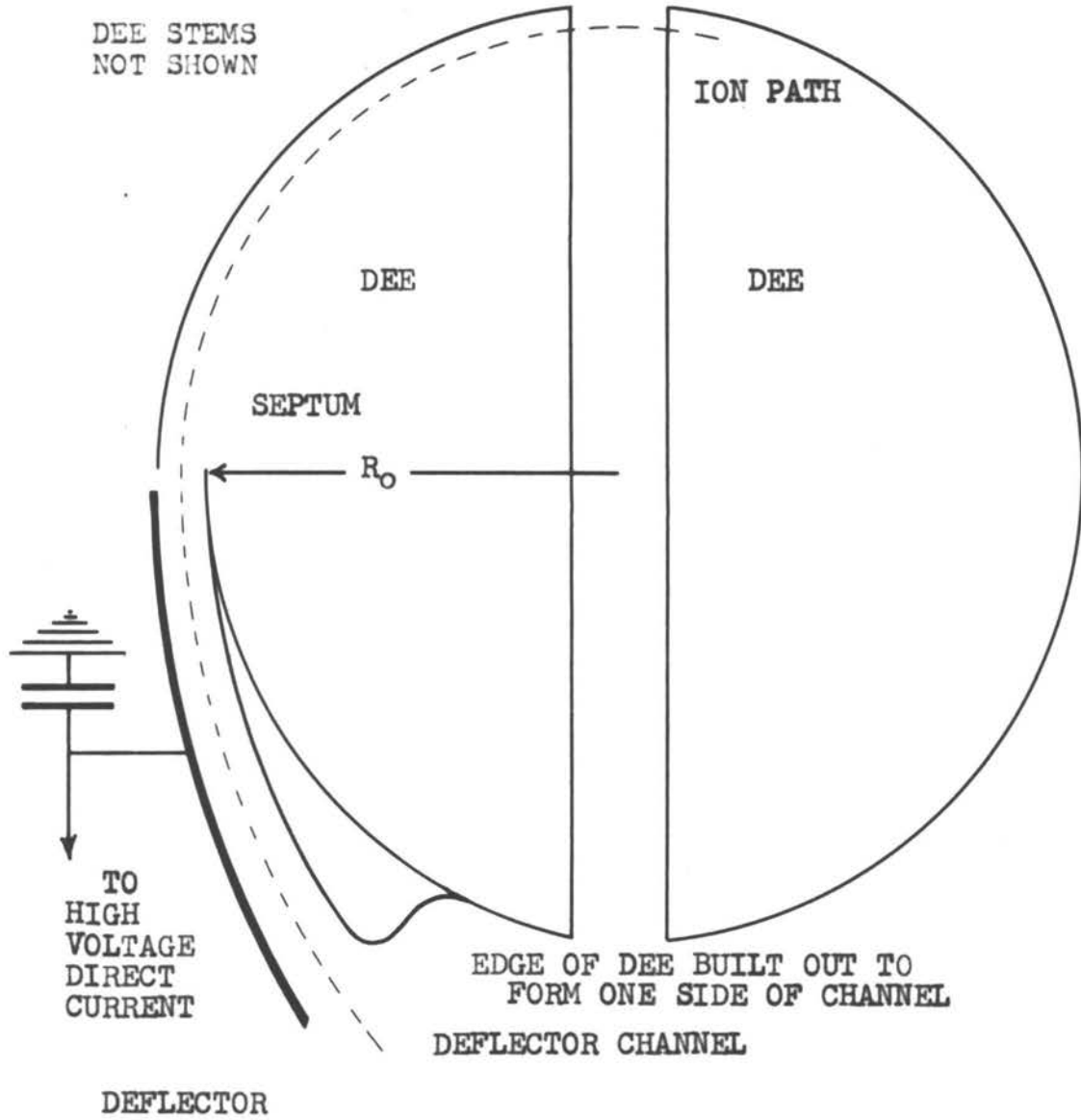


FIGURE 2.
THE R.F. DEFLECTOR

that may unbalance the R.F. tank circuit, by the addition of a strip of metal with the same capacitance as the deflector to the other dee. The use of an R.F. deflector requires more power input to the dees than a machine of similar size with a D.C. deflector.

CHANNEL WIDTH CONSIDERATIONS

The force on an ion of mass m , with charge q , moving with velocity v in a plane perpendicular to a uniform magnetic field will be perpendicular to the ion's direction and to the magnetic induction B . Therefore, the force cannot change the magnitude of the velocity, but only its direction and will be a centripetal force that produces a motion in a circular path of radius R . This can be written in gaussian units by dividing electromagnetic terms containing q by c , which has the magnitude of the velocity of light, thus

$$(1) \quad \frac{mv^2}{R} = \frac{qvB}{c}$$

As the ion is being accelerated, it will trace out a spiral path. Every time the ion gains velocity as it makes a revolution in the machine, the radius of its path will increase by an increment dR . As a group of these ions is nearing the exit radius (the radius at which the ions are withdrawn from the cyclotron through the deflector channel) they will follow a path not unlike the grooves on a phonograph record (see Figure 5); ions in adjacent orbits differ in both energy by an amount dW and radius by an amount dR . The width of the ion beam is comparable to the distance between turns dR and the entrance to the deflector channel should be comparable in width to the width of the beam.

The quantity dR can be evaluated using equation (1) and a knowledge of exit radius values of the quantities involved in the final

form of dR . Writing equation (1) again

$$(1) \quad \frac{mv^2}{R} = \frac{qvB}{c}$$

and multiplying both sides by R/v , the momentum p of the ion is obtained as

$$(2) \quad p = mv = \frac{BqR}{c} .$$

The kinetic energy W can be expressed, using the momentum, as

$$(3) \quad W = \frac{p^2}{2m} = \frac{B^2 q^2 R^2}{2mc^2} \quad ^3$$

To find the separation between the last ion path and the next to the last ion path, equation (3) is differentiated with respect to R , obtaining

$$(4) \quad dW = \frac{B^2 q^2 R^2}{2mc^2} \left(\frac{2 dR}{R} \right) .$$

Dividing equation (4) by equation (3),

$$(5) \quad \frac{dW}{W} = \frac{2 dR}{R} .$$

³ In the case of deuterons at an energy of 7.5 Mev the classical formula used here results in an error of only 0.19 per cent (as compared with the correct relativistic formula).

Multiplying equation (5) by $R/2$, dR is found to be proportional to the ratio of the change in energy of the ion during the last revolution dW , to the total energy W , and proportional to the exit radius, or

$$(6) \quad dR = \frac{dW}{2W} R .$$

The maximum value possible for dR can be obtained by assuming that the ions cross the gap between the dees when the potential difference is the maximum applied, or 100,000 volts. Since they cross the gap twice in one revolution, the value of dW will be 0.2 Mev. If the total energy of the ions at a radius of 16 inches (in a magnetic field of 14,000 gauss) is 7.5 Mev, dR would be

$$(7) \quad dR = \frac{0.2 \text{ Mev}}{2 (7.5 \text{ Mev})} (16 \text{ inches}),$$

$$= 0.213 \text{ inch}.$$

Thus, if the separation between the septum and the deflector is 0.21 inch, a beam of the maximum width expected at the exit radius could enter the deflector.

Actually there are other considerations that enter into the evaluation of the deflector spacing. At the 16 inch radius, the ions cross the gap between the dees when the potential difference is much less than 100,000 volts (the ions are said to be out of "phase" with the dee supply voltage). This condition will be discussed in more

detail in the next section; however, it is sufficient to note at this time that this condition of the ions being out of phase will not cause the value that was determined to be the maximum separation between ion orbits to be larger than the calculated value.

A second consideration is the realization that the ions at the 16 inch radius will probably not all have the same energy. If at a given instant the R.F. voltage on the dees is not constant along the edge, or if the magnetic field has azimuthal variation, the center about which the positive ions move may itself move along a line or a curve. Just how much this will affect the energy distribution in the deflected beam will have to be determined when the cyclotron is in operation. However, the spread in the energy of the 21 Mev emergent beam from the cyclotron of the University of Washington is approximately one Mev as reported by Harlow (6, p. 39). It may be possible for ions with quite a spread in energy to enter the channel with a 0.21 inch separation at the septum, but due to the fact that this beam will spread, the channel will have to be wider at its exit than where the ions pass the septum edge.

The spreading of the beam, because of the inhomogeneity of energy in the beam entering the channel, is the result of ions with different energies traveling with different radii in the magnetic field. The ions with a higher energy will travel in a straighter path. Another cause of the beam spreading in the channel is that the magnetic field is falling off rapidly in the region of the deflector, so that the ions in the outer part of the finite exit beam are in a

lesser field than those ions on the inside and therefore the outer ions will travel in a straighter path.

Information from descriptions of the spreading of deflector channels in other cyclotrons indicates that for a deflector extending over an arc of 60 degrees, the spacing at the exit should be approximately twice the spacing at the septum, and for a deflector subtending 90 degrees, this should be increased to about three times the spacing at the septum. This observation is supported by the recommendation made by Kruger, et al., (11, p. 335). A method of finding a function describing the changing deflector spacing similar to that shown by Neher (24, p. 28) will now be given.

The ions will follow approximately a circular path while traveling through the channel, a fact that will be confirmed after the path of the ions through the channel and out of the vacuum chamber is plotted. This will allow the deflector to have the shape of a segment of a circle, which is convenient to construct. A deflector channel spreading at the exit to twice the channel width at the septum may be considered as being bounded by two arcs of circles of slightly different radii (Figure 3). S , the deflector spacing, will be a function of α . The construction in Figure 3 is for the purpose of determining the function $f(\alpha)$.

Let the distance between the centers of the two circles with centers at O and O' , be represented by a , so that

$$(8) \quad r_2^2 = a^2 + (r_1 + S)^2 - 2 a (r_1 + S) \cos \beta$$

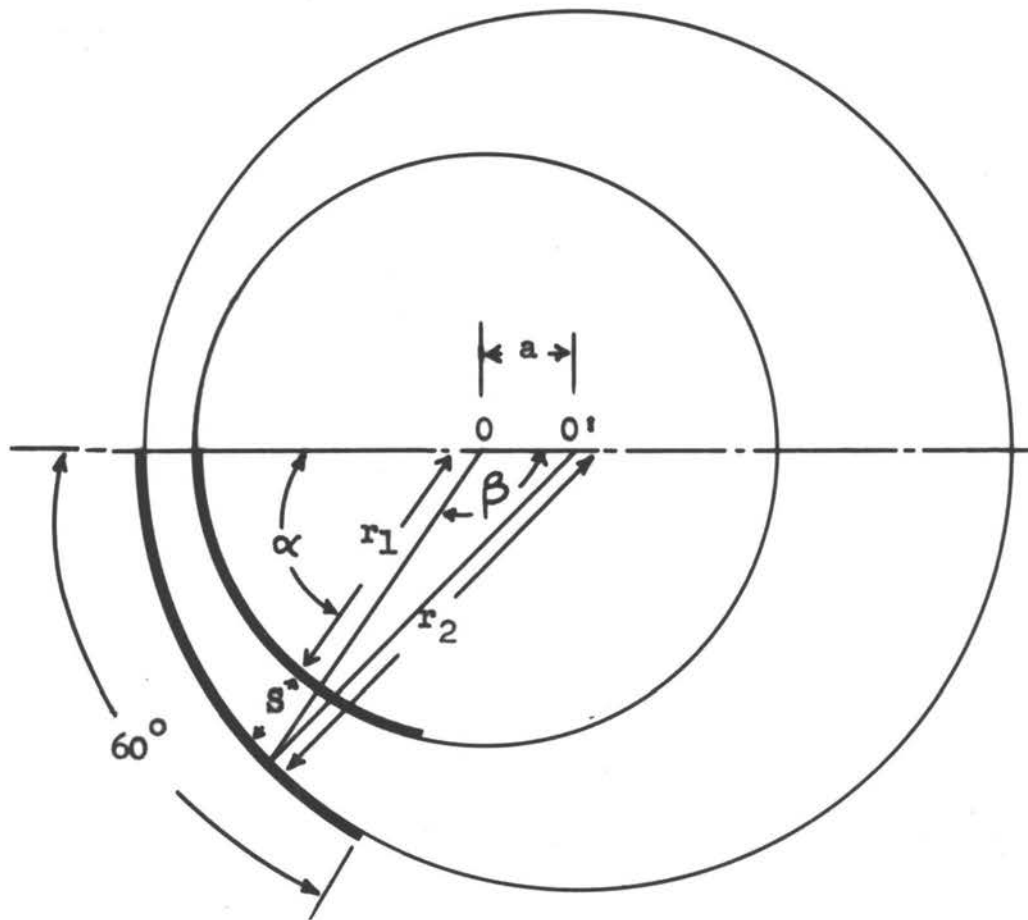


FIGURE 3.

DIAGRAM USED TO DETERMINE CHANNEL SPACING FUNCTION

Expanding the second term on the right hand side of the equation and also noticing that $\cos \beta$ is equivalent to $\cos (180 - \alpha)$ which in turn is equal to $-\cos \alpha$,

$$(9) \quad r_2^2 = a^2 + r_1^2 + 2 r_1 S + S^2 + 2 a r_1 \cos \alpha \\ + 2 a S \cos \alpha$$

Using the quadratic formula, equation (9) can be solved for S,

$$(10) \quad S = - (r_1 + a \cos \alpha) \pm \sqrt{r_2^2 - a^2 \sin^2 \alpha}$$

Since the radii involved are much larger than the distance a, the distance between the centers of the circles, a good approximation can be made by disregarding the term containing a^2 underneath the radical sign.⁴ Using the solution with the plus sign, S can be expressed as

$$(11) \quad S = r_2 - r_1 - a \cos \alpha$$

For example the values in equation (11) of a, r_1 , and r_2 for the case of the 60 degree deflector with a channel spreading from 0.21 inch at the septum to 0.42 inch at the exit, can be evaluated by considering

⁴ This amounts to an error of less than 1/4 of one per cent.

$$\alpha_1 = 0$$

$$s_1 = 0.21''$$

$$\alpha_2 = 60^\circ$$

$$s_2 = 0.42''$$

Substituting these values in equation (11) and rearranging the results slightly,

$$(12) \quad r_2 - r_1 = 0.21'' + a$$

$$r_2 - r_1 = 0.42'' + a/2$$

Solving the equations in (12) the value of a is determined as 0.42 inch, and $r_2 - r_1$ is 0.63 inch. Substituting these values in equation (11),

$$(13) \quad S = 0.63 - 0.42 \cos \alpha, \quad (\text{inches})$$

the function S representing the variation of the deflector spacing, is determined. If different deflector spacings are used, a new function describing the changing deflector width may be determined by substituting the new values in (11) and following the same procedure.

Below, the deflector is divided into 10 degree segments and the channel width S is tabulated for each 10 degree segment.

α	S (cm.)
0	0.534
10	.559
20	.610
30	.686
40	.813
50	.915
60	1.068
70	1.237
80	1.417
90	1.602

Table 1
CHANNEL SPACING

THE DEFLECTING FIELD

Ion deflection is largely dependent upon the instantaneous value of the R.F. voltage on the dee when the ion is entering the channel. The R.F. component of the deflecting field at that time is dependent upon the phase of the ion. The phase of the ion describes the difference between the time the accelerating voltage on the dee is at its maximum value and the time the ion crosses the center of the dee gap.⁵ It determines the fraction of the dee voltage that is available to the ion for energy gain as the ion crosses the accelerating gap between the dees.

The phase of the ion varies as the ion is accelerated to its final energy and will result in the ions arriving at the target in pulses. To show that the phase angle will vary it is necessary to examine equation (1). Rewriting it here for convenience,

$$(1) \quad \frac{mv^2}{R} = \frac{Bqv}{c},$$

both sides of the equation are divided by mv , obtaining

$$\frac{v}{R} = \frac{Bq}{cm}.$$

⁵ An ion crossing the dee gap when the voltage on the dees is at its maximum value will have a phase angle of 90 degrees. An ion with a phase angle of 180 degrees will undergo no acceleration as it crosses between the dees, and with a phase angle of 181 degrees the ion will undergo deceleration.

The angular velocity ω with which the ion travels in its orbit in the cyclotron is equal to v/R . Thus

$$\omega_{\text{ion}} = \left(\frac{B}{c} \right) \left(\frac{q}{m} \right)$$

It is apparent that the ion will travel with an angular velocity determined by the instantaneous values of the terms in the right hand side of the equation for ω . In the previous section it was observed that the relativistic change in mass at the deuteron energy of 7.5 Mev was negligible so that the term q/m will be substantially constant. However, the magnetic field in the cyclotron is not strictly constant. From the center of the field out to the exit radius, the magnetic field decreases by 2 to 3 per cent. Thus the ion will travel with a slightly greater angular velocity at the center of the cyclotron than it will at the edge (2, p. 60).

On the other hand, the dee voltage frequency is very nearly constant, being determined by the inductance and capacitance of the dee system. The result of this is that the angular frequency of the ion will not be in phase with the voltage applied to the dee at all times. At the entrance to the channel the ion will lag behind in phase with the dee voltage, (i.e. have a phase angle greater than 90 degrees). Harlow (6, p. 26) estimates that the maximum phase angle for the ion beam of the University of Washington cyclotron is about 170 degrees. Neher (24, p. 8) reported in a letter to Kruger that a maximum phase angle of 170 degrees had been measured in the

pre-1949 60-inch cyclotron at the University of California, for an ion pulse extending over an arc of 40 degrees. (The mean ion is located in the portion of the ion pulse containing the maximum number of ions. In a beam with a pulse of ions covering a 40 degree arc, and with a maximum phase angle of 170 degrees, the mean ion will have a phase angle of 150 degrees.)

The phase of the ion is important in its deflection from another consideration. Ions with large phase angles up to 175 degrees will be deflected more because they are in a slightly higher average deflecting field. Ions with smaller phase angles will be deflected less. For this reason, ions with phase angles between 150 and 175 degrees will have to have less energy to pass through the channel than ions with phase angles less than 150 degrees. In contradiction to this fact is that, those ions with higher energies will travel around the cyclotron more times than ions with less energy, and so they will have a larger phase angle. The result of this is that the deflector will exhibit the effect shown by mass spectrometers, i.e. the deflector will be selective to energy. For this reason, the energy distribution of the ions at the target due to phase should be small.

Figure 4 is a section of the vacuum chamber and dees at the median plane. The ion beam, in leaving the cyclotron, must pass through the two points: (1) the entrance to the deflector channel, and (2) the point previously determined for the ion beam to leave the vacuum chamber.

The choice of the first point, the entrance to the channel, is dependent upon the following considerations: (a) limitations imposed upon the placement of the entrance to the channel because of the connection of the dee stem to the dee, and (b) the voltage desired on the deflector, which depends upon the azimuthal location of the deflector. The construction of the dees may limit the position of the entrance to the channel to an angle greater than 80 or 90 degrees past the dee edge.

The azimuthal location of the deflector can be varied to change the average voltage on the deflector. The maximum voltage on the deflector occurs, for an ion with a phase angle of 170 degrees, when the ion is 100 degrees past the dee edge. For an ion with a phase angle of 150 degrees, the maximum voltage on the deflector will occur when the ion has traveled 120 degrees past the dee gap. To obtain the maximum deflecting field from the voltage applied to the dees, the entrance of the channel should be located at the position of the mean ion when the dee voltage is maximum.

Inspection of Figure 4 will indicate that the ion beam must leave the vacuum chamber at a point as near to the corner as convenient so that use may be made of the maximum available space between the beam and the magnetizing-coil cooling-air duct for equipment. The deflecting field must be strong enough to pull the ions out to this point.

When the ion enters the channel, it is affected by the force from the magnetic field. The effect of the electrostatic force on

Scale: 1 inch = 1/16 inch

22

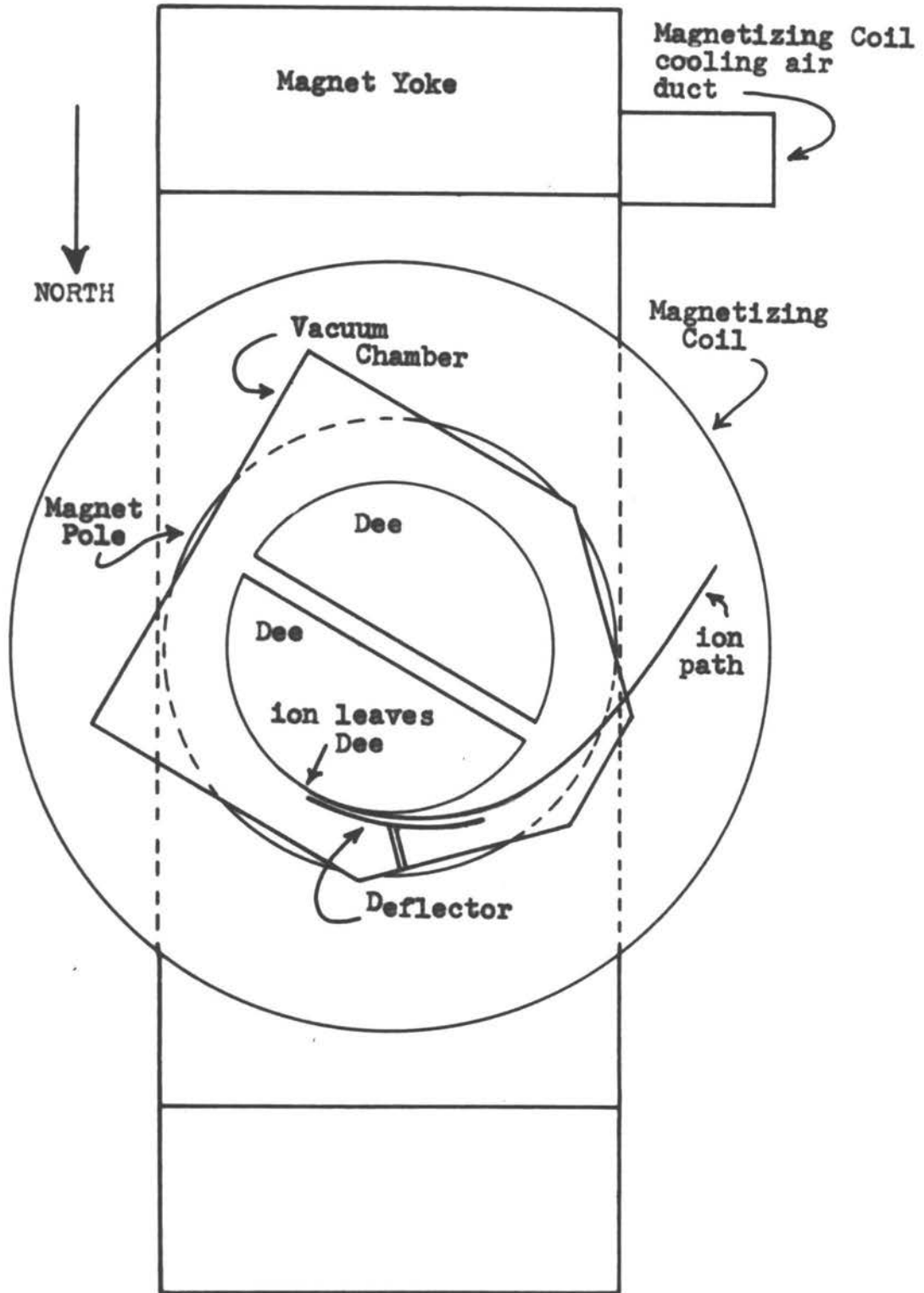


Figure 4.

Sectional view of Cyclotron from air gap of Magnet.

the ion is that the radius of the path of the ion is increased. Instantaneously the ion has not had time to move along its new path so that its new radius must be along the line of the ion path's radius before it entered the deflector, i.e. its new radius must pass through the center of curvature of the old path. If the electrostatic deflecting field was constant the ion would move along the arc described by the new radius. However, the voltage on the deflector changes as the ion passes along its length, so that the force on the ion is not constant; also, the ion now moves through a decreasing magnetic field. The radius of curvature is therefore continually changing and it is necessary to compute the radius of curvature at successive intervals throughout the channel. The determination of the field necessary to bring the ion out of the cyclotron will now be discussed, and the computation of the path of the ion from the cyclotron will be done in the next section.

When the ion enters the deflecting channel, it feels an electric force E_q , as well as the magnetic force upon it. If this force is in the plane of motion, the cyclotron equation (1) is modified to include this additional force. The equation of motion becomes the Lorentz equation,

$$(14) \quad Bqv/c - E_q = mv^2/R_1 ,$$

where R_1 is the instantaneous radius of the ion as it enters the channel. Now it will be necessary to distinguish between the radius R

that occurs as a variable, e.g. equation (1), the exit radius R_0 , a constant that is the distance from the entrance of the deflector to the center of the cyclotron magnet, and the radii $R_1, R_2, R_3 \dots, R_7$, which are the instantaneous radii of the mean ion at points, differing by an arc of 10 degrees within the channel.

From equation (14)

$$(15) \quad E = \frac{1}{q} \left[\frac{Bqv}{c} - \frac{mv^2}{R_1} \right] .$$

This may be rewritten in terms of the kinetic energy of the ion W , by letting

$$(16) \quad 2W = mv^2$$

and substituting for v in equation (15),

$$(17) \quad v = \sqrt{\frac{2W}{m}} .$$

Making this substitution,

$$(18) \quad E = \frac{1}{q} \left[Bq \sqrt{\frac{2W}{mc^2}} - \frac{2W}{R_1} \right] .$$

The kinetic energy of the ion at any radius, R , is given in equation (3). At the exit radius R_0 , the kinetic energy is found to be

$$(19) \quad W = \frac{B_o^2 q^2 R_o^2}{2mc^2},$$

where B_o is the magnetic induction at the deflector entrance. E can be expressed in exit radius conditions as

$$(20) \quad E = \frac{1}{q} \left[\frac{B B_o q^2 R_o}{e^2 m} - \frac{B_o^2 q^2 R_o^2}{m c^2 R_1} \right],$$

$$(21) \quad E = \frac{B B_o q R_o R_1 - B_o^2 q R_o^2}{R_1 m c^2}.$$

This may be reduced to a simpler form by dividing both numerator and denominator by

$$(22) \quad B_o^2 q R_1 R_o,$$

obtaining,

$$(23) \quad E = \frac{\left[\frac{B}{B_o} - \frac{R_o}{R_1} \right]}{\frac{mc^2}{B_o^2 q R_o}}.$$

Evaluating equation (23) at the entrance to the deflector ($B = B_0$),

$$(24) \quad E = \left[1 - \frac{R_0}{R_1} \right] \frac{B_0^2 q R_0}{mc^2} .$$

For deuterons with a kinetic energy of 7.5 Mev:

$$m = 3.34 \times 10^{-24} \text{ gram,}$$

$$c = 3 \times 10^{10} \text{ centimeters per second,}$$

$$B_0 = 13,870 \text{ gauss,}$$

$$q = 4.8 \times 10^{-10} \text{ stat coulomb}$$

$$R_0 = 16 \text{ inches,}$$

and E will be in electrostatic volts per centimeter.

$$(25) \quad E = \left[1 - \frac{16}{R_1} \right] \frac{(13,870)^2 (4.8 \times 10^{-10}) (16) (2.54)}{(3.34 \times 10^{-24}) (3 \times 10^{10})^2}$$

$$(26) \quad E = \left[1 - \frac{16}{R_1} \right] \frac{10^4}{8} \quad (\text{statvolts per centimeter}).$$

The direction of R_1 is already known since R_1 , the radius of curvature as the ion enters the deflector, will be along the line

of the pre-entrance radius. The magnitude of R_1 can be estimated roughly from the scale diagram in Figure 5. Placing the pivot point of a compass on the line of R_1 at such a point that the pencil will swing through the entrance to the deflector channel and the point of the ion exit from the vacuum chamber, the distance is measured between the deflector entrance and the pivot point with a scale. This value of R_1 in equation (26) will give the approximate magnitude of the deflecting field necessary to start the ion on its path from the cyclotron.

Table (2) has been tabulated listing the approximate static deflecting field necessary to deflect the mean ion at various phase angles for different positions of the entrance to the deflector channel. The estimated instantaneous radius of the mean ion as it enters the deflector and the D.C. voltage necessary to produce the electrostatic deflecting field is also listed. Since the radius of the ion as it enters the channel is estimated by considering the total ion path instead of just the path in the channel, the resulting values for the D.C. bias may be considerably higher than the actual value. The purpose of the table is to serve as a rough guide to use in the process of "sighting in" the deflector. The values in the table may be larger than needed by 10,000 volts.

Scale
1.0 inch = 0.125 inch

Outline of
Vacuum Chamber

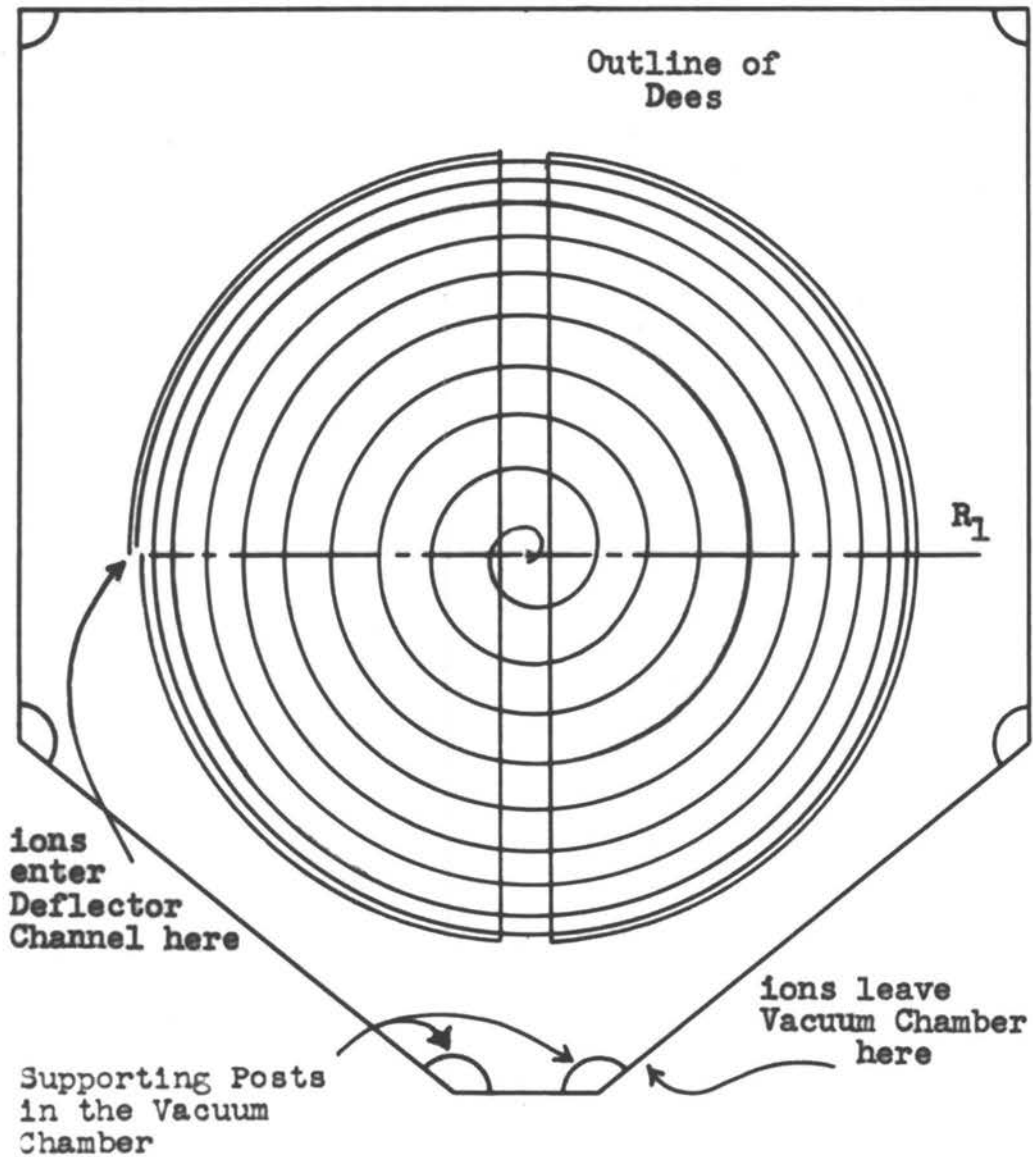


Figure 5.

Scale diagram of vacuum chamber and dees.

phase angle	deflector entrance	ion radius	deflecting field	deflector bias
ϕ degrees	θ degrees	R_1 inches	E ($\frac{\text{statvolts}}{\text{cm}}$)	V_{DC} volts
160°	70°	20.8	298	7,400
	80	21.3	311	6,800
	90	22.2	348	7,800
150°	70°	20.8	298	13,600
	80	21.3	311	11,700
	90	22.2	348	12,500
140°	70°	20.8	298	20,700
	80	21.3	311	17,900
	90	22.2	348	17,400

APPROXIMATE VALUES OF THE RADIUS OF CURVATURE
OF THE ION PATH AT THE ENTRANCE TO THE CHANNEL

Table 2

The deflecting field E , will be a function $E(\theta, t)$ of the angular distance moved in the deflector channel θ , for a deflector channel of varying width, and of t for a time dependent voltage on the dees. The deflecting voltage is composed of the voltage on the dee $V_0 \sin(\omega t + \phi - \pi)$, and the D.C. bias voltage V_{DC} , added to make up the difference between the instantaneous dee voltage and the voltage required to produce E . The deflecting voltage V is thus

$$(27) \quad V = V_{DC} + V_0 \sin(\omega t + \phi - \pi)$$

where ω is the angular frequency of the dee voltage and t is the time spent in the deflector. The time dependence may be eliminated since

$$(28) \quad \omega t = \theta .$$

θ is the angle past the center of the dee gap, and ϕ is the phase angle of the ion. The deflecting field is

$$(29) \quad E = \frac{V_{DC} + V_0 \sin(\theta + \phi - \pi)}{300 S}$$

and S is the deflector channel width function from equation (14) with α replaced by $(\theta - \pi/2)$, and converted to centimeters. Similar forms of the deflecting field are given in (6, p. 28) and (24, p. 18).

The value of the D.C. voltage on the deflector is determined by establishing the deflecting field E , necessary to remove the ion from the vacuum chamber from Table 2, or with equation (26). With a given ion phase ϕ , and a given angle θ , substitutions may be made in equation (29), and the value of V_{DC} necessary to produce E determined when $V_0 = 50,000$ volts.

CALCULATION OF THE PATH OF THE ION

The Lorentz equation (14) describes the forces acting on an ion in the deflector channel. Rewriting it here for convenience,

$$(30) \quad mv^2/R_i = Bqv/c - qE .$$

The calculation of the path of the ion involves the instantaneous ion path radius R_i , not the distance R from the center of the cyclotron magnet, which may not even lie along the same line. Because the forces on the ion in the channel are continuously changing, an exact plot of the ion path cannot be made and approximations are appropriate. It is convenient to divide the path in 10 degree segments, and compute for each segment an R_i from the information gained from evaluating the instantaneous radius of the previous segment. The error involved here is small and will be discussed in detail later. As large a change of the instantaneous radius as 5% will result in a change in the path of the ion, with respect to the center of the cyclotron, of only a fraction of a per cent.

The steps necessary to obtain equation (23)

$$(31) \quad E = \left[\frac{B}{B_o} - \frac{R_o}{R_i} \right] \frac{B_o^2 q R_o}{mc^2}$$

were described in the previous section. Solving for R_i , and using the calculation for the constant term from equation (26),

$$(32) \quad R_1 = \frac{R_0}{\frac{B}{B_0} - 8 \times 10^{-4} E}$$

A step by step computation for each segment of the deflector may be made using this formula. An instantaneous radius is computed for each segment and thereby, a plot can be made of the path of the ions from the cyclotron.

The values of B to use in equation (32) are obtained from the two graphs in Figures 6 and 7.⁶ The first graph covers the range of the radius in which the deflector is located, and in which the value of the magnetic induction may be determined quite accurately. The second graph contains the data plotted on the first graph on a smaller scale and is extrapolated over the region from 19 inches to 22 inches.

(No data has been taken for this region yet.) The extrapolation in this region was made by taking the tangent to the curve at the radius for which the last measurement of the magnetic induction was made. This extrapolation gives the maximum magnetic induction for the cyclotron magnet that can be expected for this range of the radius. It can be compared with the complete plots of magnetic fields in the notes obtained by Gallop (5, pp. 5, 40, 52) and the plot of the University of California 60 inch cyclotron magnet (24, p. 14). The values of the magnetic induction obtained in the region of the

⁶ The information for these graphs was obtained from the data taken from the measurements made on the cyclotron magnet by D. B. Nicodemus and D. J. Bates.

extrapolation allow the computation of the approximate path of the ion from the vacuum chamber. This approximation is fairly accurate since the results from using the probable values for the magnetic induction instead of the extrapolated values has very little effect in changing the radius of curvature in this range. The error involved from using the extrapolated values will be that the ion beam will be brought out slightly further than calculated. This may be corrected experimentally when the cyclotron is in operation by decreasing the value of the D.C. bias applied to the deflector.

The values of $(8 \times 10^{-4} E)$ used in equation (32) for the following calculations are listed in Table 3. These are computed from equation (29) at 10 degree intervals in the deflector channel. Given a value of θ , and locating the deflector entrance at 70, 80, or 90 degrees past the gap between the dees, a value of V_{DC} can be determined from Table 2. The values of E are then determined, starting at the entrance and using the value of S for this position from Table 1, and continuing the computation every ten degrees along the length of the deflector.

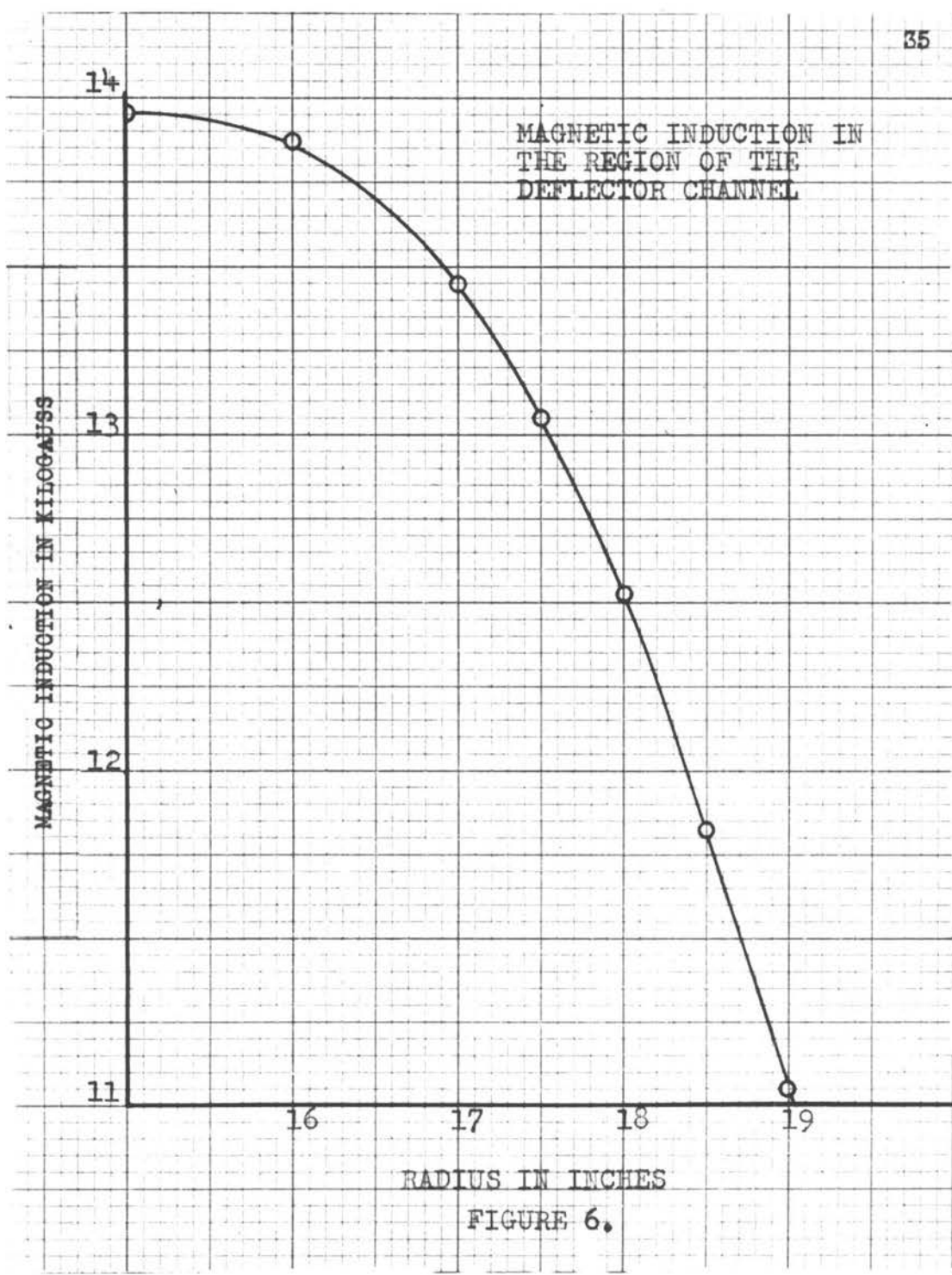


FIGURE 6.

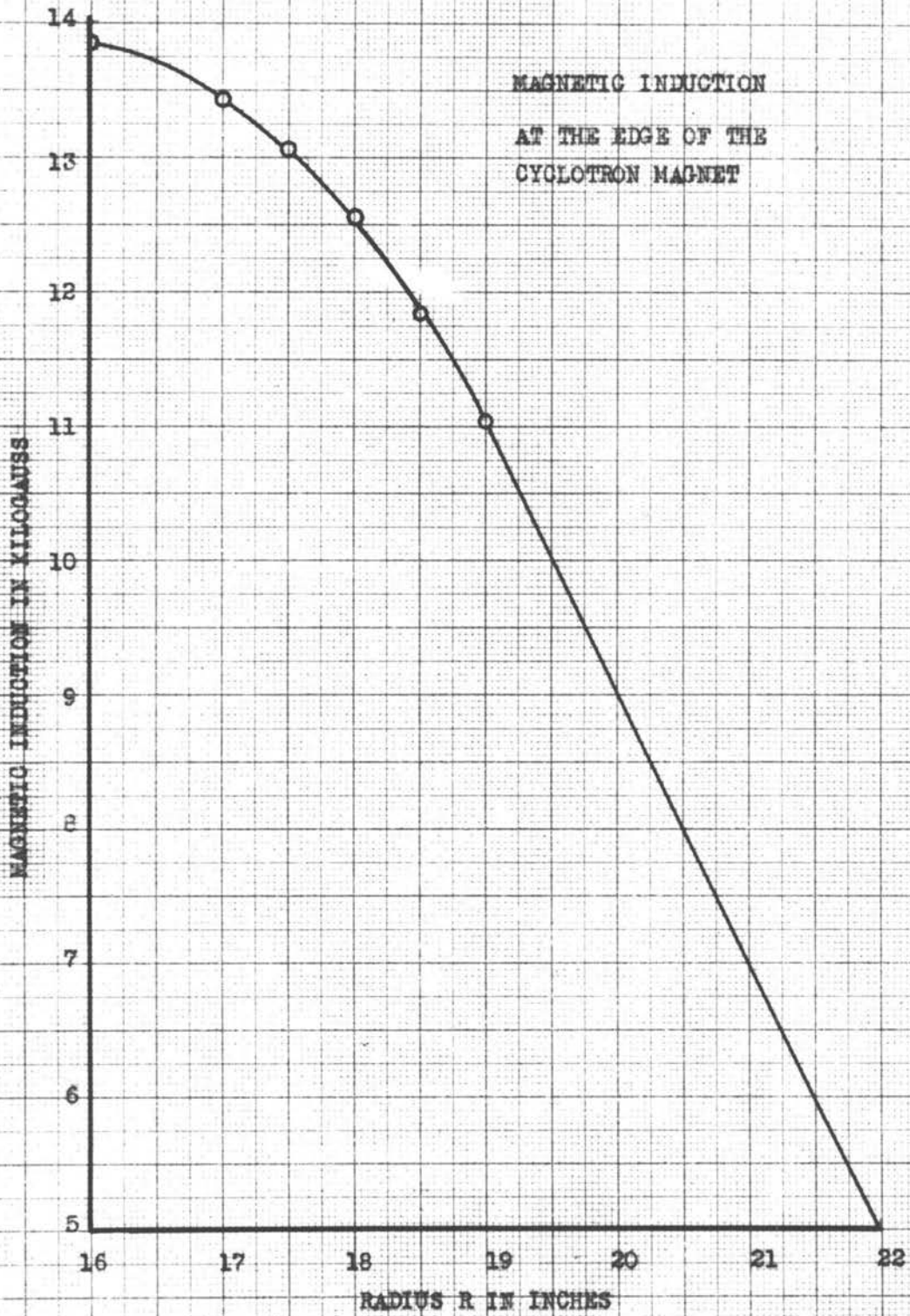


FIGURE 7.

VALUES OF $8 \times 10^{-4} E$

37

θ degrees	$8 \times 10^{-4} E$	θ degrees	$8 \times 10^{-4} E$
90	0.266	80	0.191
100	0.271	90	0.206
110	0.258	100	0.205
120	0.233	110	0.191
130	0.194	120	0.164
140	0.166	130	0.143
150	0.133	140	0.117

For path plotted in
Figures 8, 13

For path plotted in
Figure 9

I	θ degrees	$8 \times 10^{-4} E$	J	θ degrees	$8 \times 10^{-4} E$
	90	0.316		80	0.271
	100	0.319		90	0.271
	110	0.302		100	0.258
	120	0.299		110	0.233
	130	0.227		120	0.194
	140	0.195		130	0.165
	150	0.181		140	0.133

For path plotted in
Figure 10

For path plotted in
Figure 11

Table 3

H	θ degrees	$8 \times 10^{-4} E$
	90	0.320
	100	0.310
	110	0.281
	120	0.240
	130	0.191
	140	0.155
	150	0.162

For path plotted in
Figure 12

Table 3 (Continued)

The procedure used to plot the path of an ion, with a phase angle of 150 degrees and entering the channel 90 degrees past the dee gap, will now be followed. In Table 2, the approximate value of the D.C. bias needed to bring the ion beam out at a point just south of the supporting post is listed as 12,500 volts. A bias of slightly less than this of 10,000 volts will be added to a deflector extending over an arc of 60 degrees.

On the scale drawing of the dees and vacuum chamber, (Figure 8) the center of the cyclotron magnet is located, and the arc from the entrance of the channel to the exit from the vacuum chamber is divided into 10 degree segments. (In Figure 8, these 10 degree divisions are denoted by small circles just above the ion path.) From the graph in Figure 6 the values of B are obtained; from Table 3, values of $8 \times 10^{-4} E$ are obtained. Since the definition of B_0 is the value of the magnetic induction at the exit radius, the initial value of B/B_0 is 1. These values in equation (32) give

$$(33) \quad R_1 = \frac{16.00}{1 - 0.266}$$

$$(34) \quad R_1 = 21.8 \text{ inches}$$

A point along a line through the entrance to the channel and the center of the cyclotron, (line A-A' in Figure 8) is located a distance R_1 or 21.8 inches from the path of the ion as it enters the channel.

A 10 degree arc is constructed about this point starting at the entrance to the deflector channel. The distance R (from the center of the cyclotron magnet out to the ion path) is measured at the end of the first 10 degree segment, i.e. 10 degrees past the entrance to the channel. This value of R is used in the graph in Figure 6 to determine the value of the magnetic induction at the location of the ion path. In Table 3 the value of E at 100 degrees is obtained. Substituting these values in equation (32),

$$(35) \quad R_2 = \frac{16.00}{0.729},$$

$$(36) \quad R_2 = 22.0 \text{ inches} .$$

The center of the next 10 degree arc is located at a point 22.0 inches from the ion path, along a line through the end of the first segment (the 100 degree division) and its center of curvature (point B). (This is along line B-B' in Figure 8.) After constructing this arc, the distance R is measured from the center of the magnet to the ion path at the 110 degree division. The value of B from Figure 6 and the value of E listed for 110 degrees in Table 3 are put in equation (32) to obtain

$$(37) \quad R_3 = \frac{16.00}{\frac{13,820}{13,870} - 0.258},$$

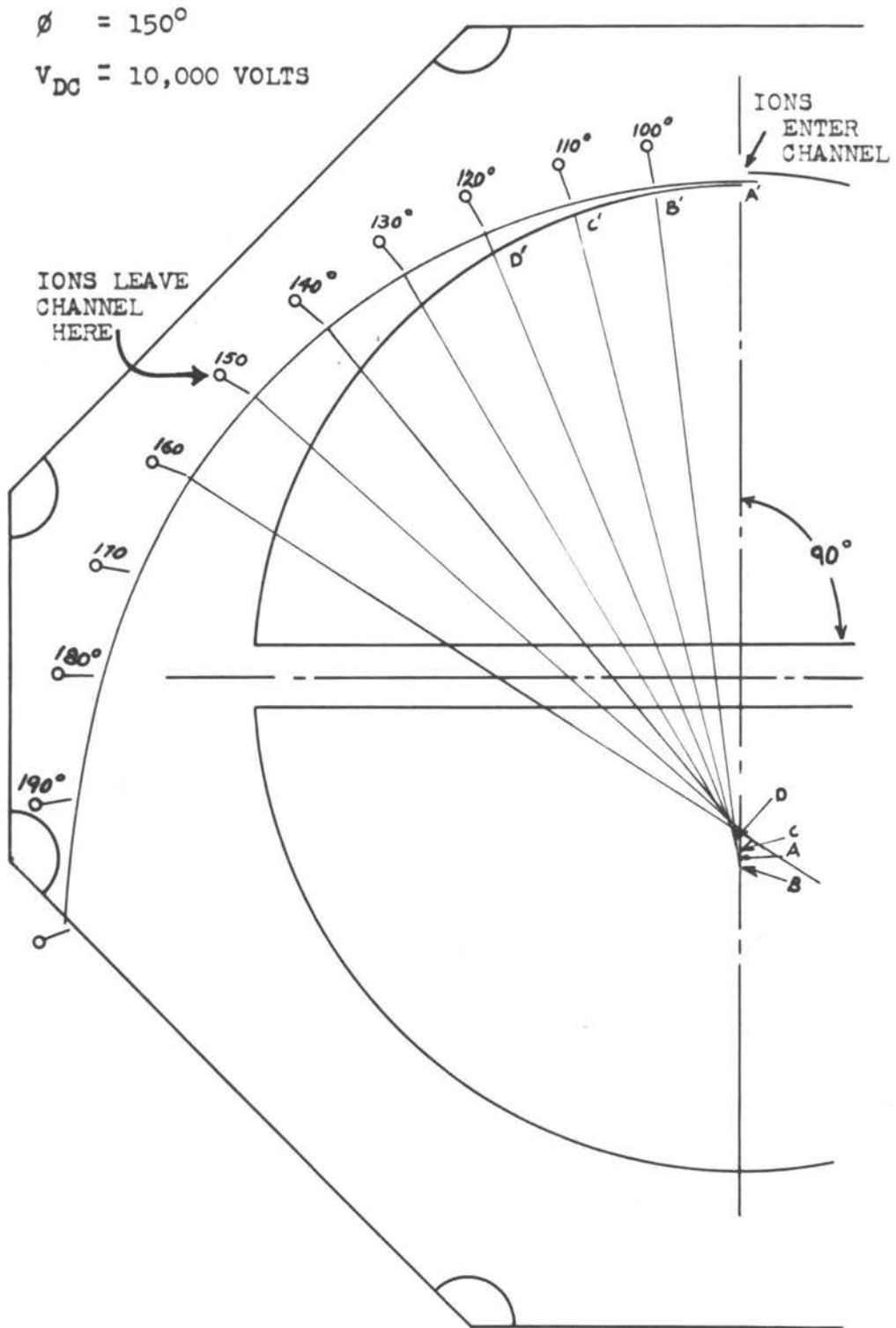


FIGURE 8.
 CONSTRUCTION OF THE ION PATH

$$(38) R_3 = \frac{16.00}{0.998 - 0.258}$$

$$(39) R_3 = 21.6 \text{ inches .}$$

The same process used above is used to determine the location of the center of the next 10 degree arc.

At 120 degrees, the distance from the ion path to the center of the cyclotron (R) was measured as 16.6 inches. The value for B determined from Figure 6 is 13,660 Gauss, which gives a B/B_0 ratio of 0.985. Substituting this ratio and the value from Table 3 at 120 degrees of 0.233, in equation (32) gives

$$(40) R_4 = \frac{16.00}{0.985 - 0.233} ;$$

$$(41) R_4 = 21.3 \text{ inches.}$$

A point 21.3 inches is measured back from the ion path at the 120 degree mark along line D-D'. This is the center of curvature of the segment of the ion path from 120 degrees to 130 degrees.

The values for the radii of curvature of the ion in the rest of the channel have been computed and are listed in Table 4. The procedure used to find them is the same as used to find the radii above.

Outside the deflector channel, the path of the ion may be plotted further. The value of R measured at 160 degrees is 19.1 inches. This gives a value for B as read from the extrapolated portion of the curve in Figure 7, of 10,900 gauss, and a B/B_0 ratio of 0.787. Now, since there is no deflecting field, the term involving E in equation (32) drops out leaving

$$(42) \quad R_8 = \frac{16.00}{0.787}$$

$$(43) \quad R_8 = 20.3 \text{ inches .}$$

The procedure used in locating the center of curvature is the same as above, and should be followed until the ion is out of the vacuum chamber.

Figure 9 shows the construction lines for plotting the path of an ion whose phase is 150 degrees. No D.C. voltage is needed to bring the beam out of the vacuum chamber when the entrance of the channel is at 80 degrees past the dee gap. The segments of the path between 90 degrees and 120 degrees have the same radius of curvature as do the two segments between 120 degrees and 140 degrees.

The ion path that has been plotted will closely approximate the exact path the ion will follow in the channel. Errors occurring in the computation of the first two or three radii of curvature will have a greater effect on the results than the same error made at the end of the deflector. However, the use of moderate care in making

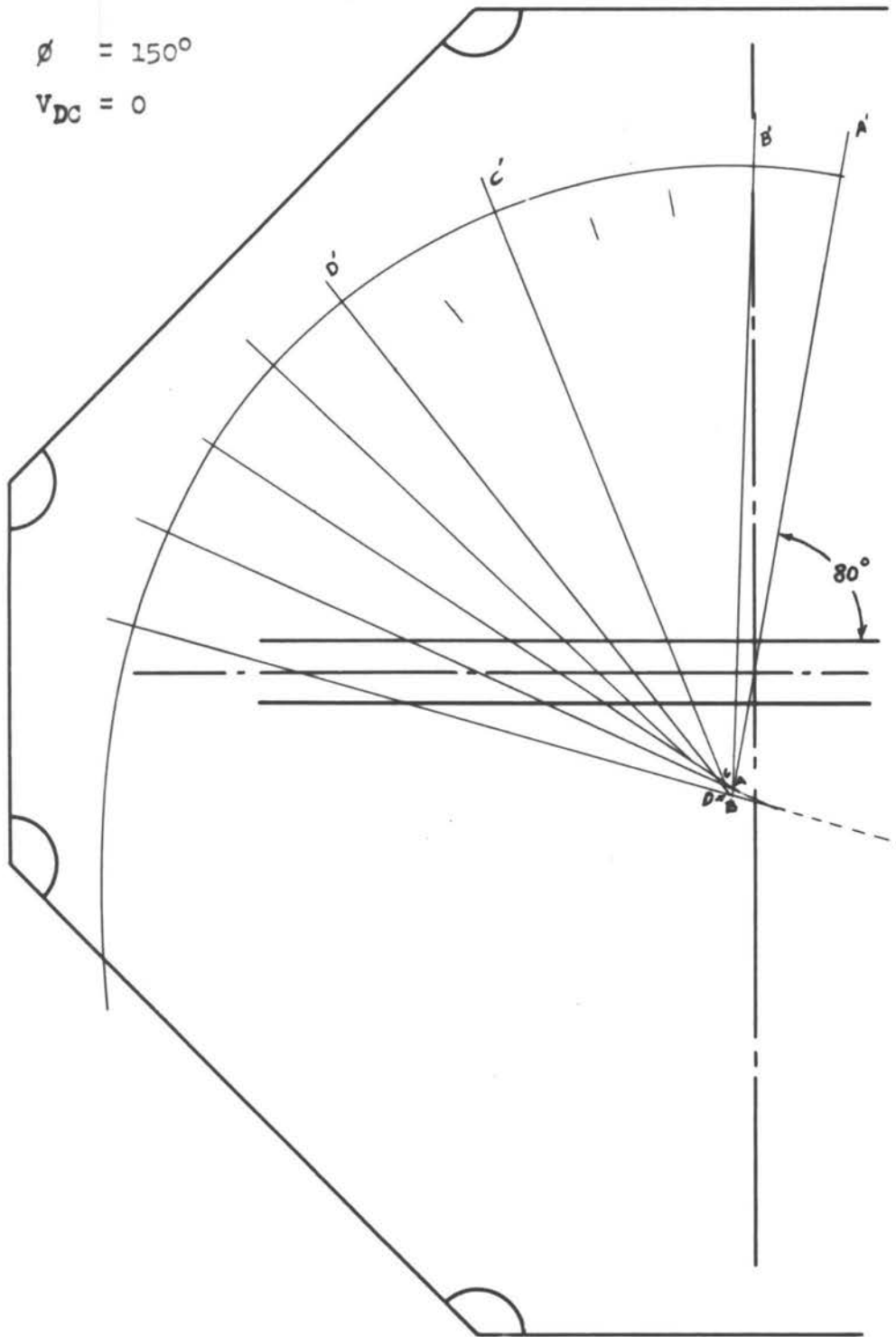


FIGURE 9.

CONSTRUCTION OF THE ION PATH

the computations will assure results accurate enough for all practical applications. Even relatively large errors in the components of equation (32) have little effect on the magnitude of the radius of curvature, and hence the path of the ion. Evidence of this may be seen in the calculation of the approximate center of curvature for the deflector.

In the construction of the sides of the deflecting channel, it would be more convenient to bend the deflector, on one side of the deflecting channel, and the back side of the dee on the other side, to the shape of a segment of a circle, than to a segment of the spiral path of the ion. It will now be shown that the path of the ion closely approximates a segment of a circle in the 60 degree arc of the deflecting channel, so the circular approximation will be quite accurate.

In Figure 10, the radial lines intersecting the ion path at 90, 110, 130, and 150 degrees have been marked as A, B, C, and D respectively. Perpendicular bisectors of cords intersecting the ion path at A-C and B-D are constructed. The point at which these two bisectors intersect is the mean center of curvature for the path of the ion in the deflecting channel. To avoid confusion in the description of this calculation, the bisectors have been labeled E-E' and F-F', their point of intersection being designated by O.

An example of how much lee-way there is in locating the center of curvature for the radii, $R_1, R_2, R_3 \dots, R_7$, and therefore, how comparatively large an error may be introduced in the magnitude of

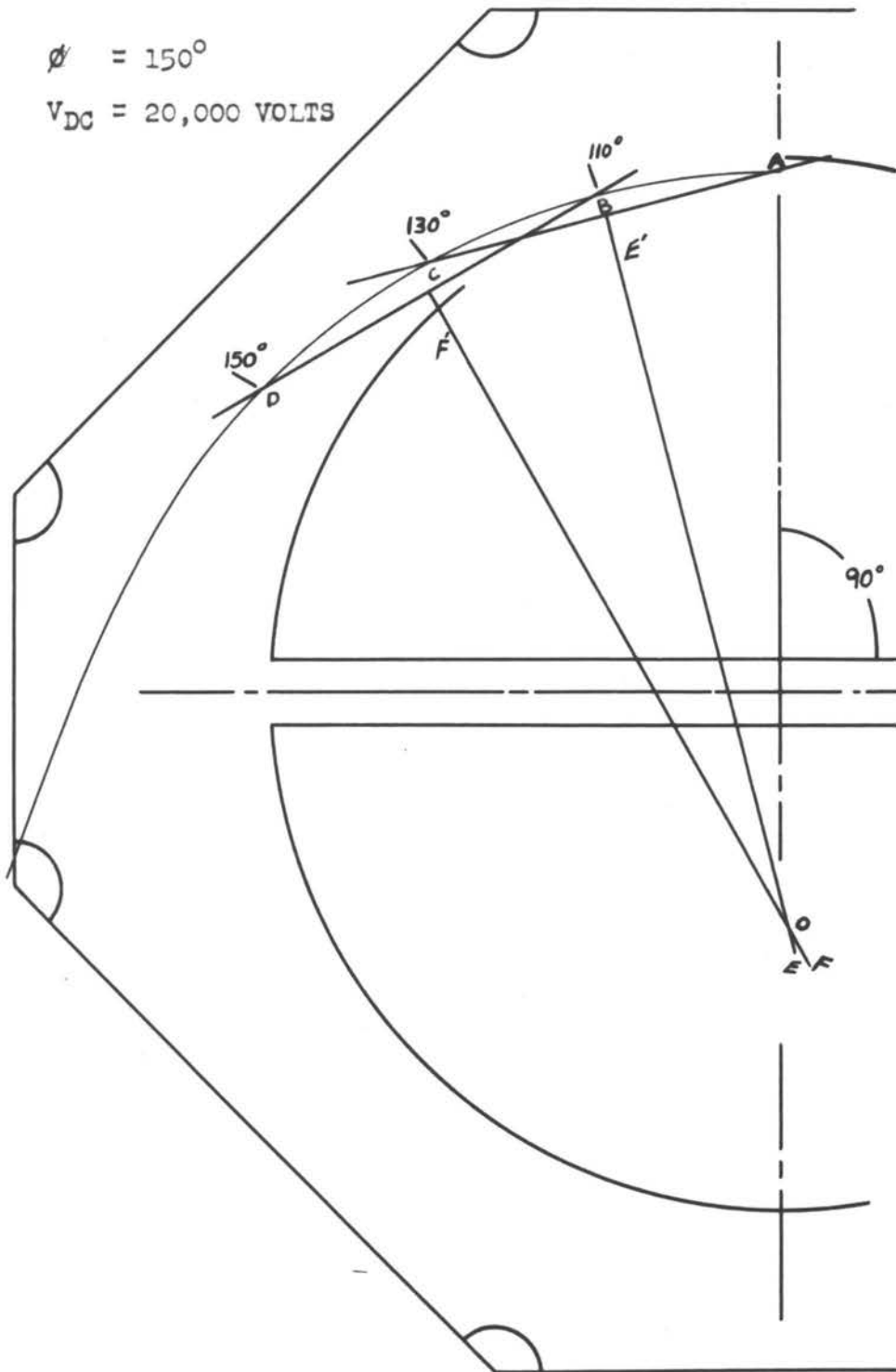


FIGURE 10.

PLOT OF THE ION PATH

these radii without affecting the path of the ion, may be seen by passing the pencil of a compass with its pivot point located at O, through A, B, C, and D. In the plots made, the trace of the pencil cannot be distinguished from the path of the ion except for a few degrees where the separation is very slight. Therefore, the path of the ion in the deflector may be approximated by a segment of a circle.

In Figure 11 the center of curvature of the ion path is shown. Labeled A'-D' and A''-D'' respectively are the edges of the deflector and the back side of the dee that form the deflecting channel. The distance between A'-A'' and D'-D'' is the spacing at the entrance and exit to the deflector channel as determined from Table 1. The center of curvature of the deflector may be determined by finding a position to locate the pivot point of a compass so that the pencil will swing through A' and D'. The center of curvature for the other side of the deflecting channel may be located by finding a point to locate the pivot of the compass so that the pencil will pass through A'' and D''. The center of curvature of the ion path is shown in Figure 11 as O, the center of curvature of the deflector is shown as O', and the center of the back side of the dee is O''.

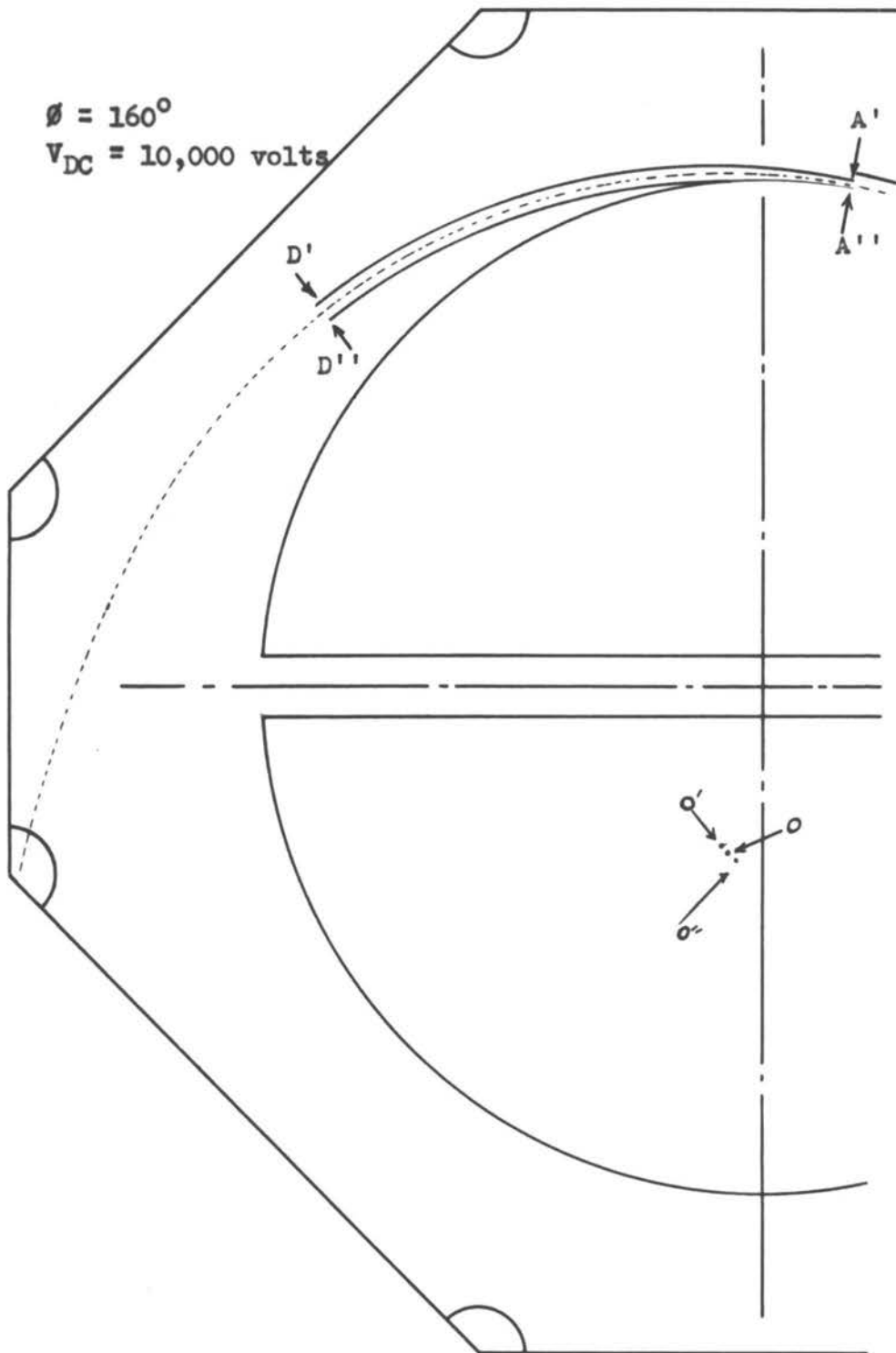


FIGURE 11.
PLOT OF THE ION PATH

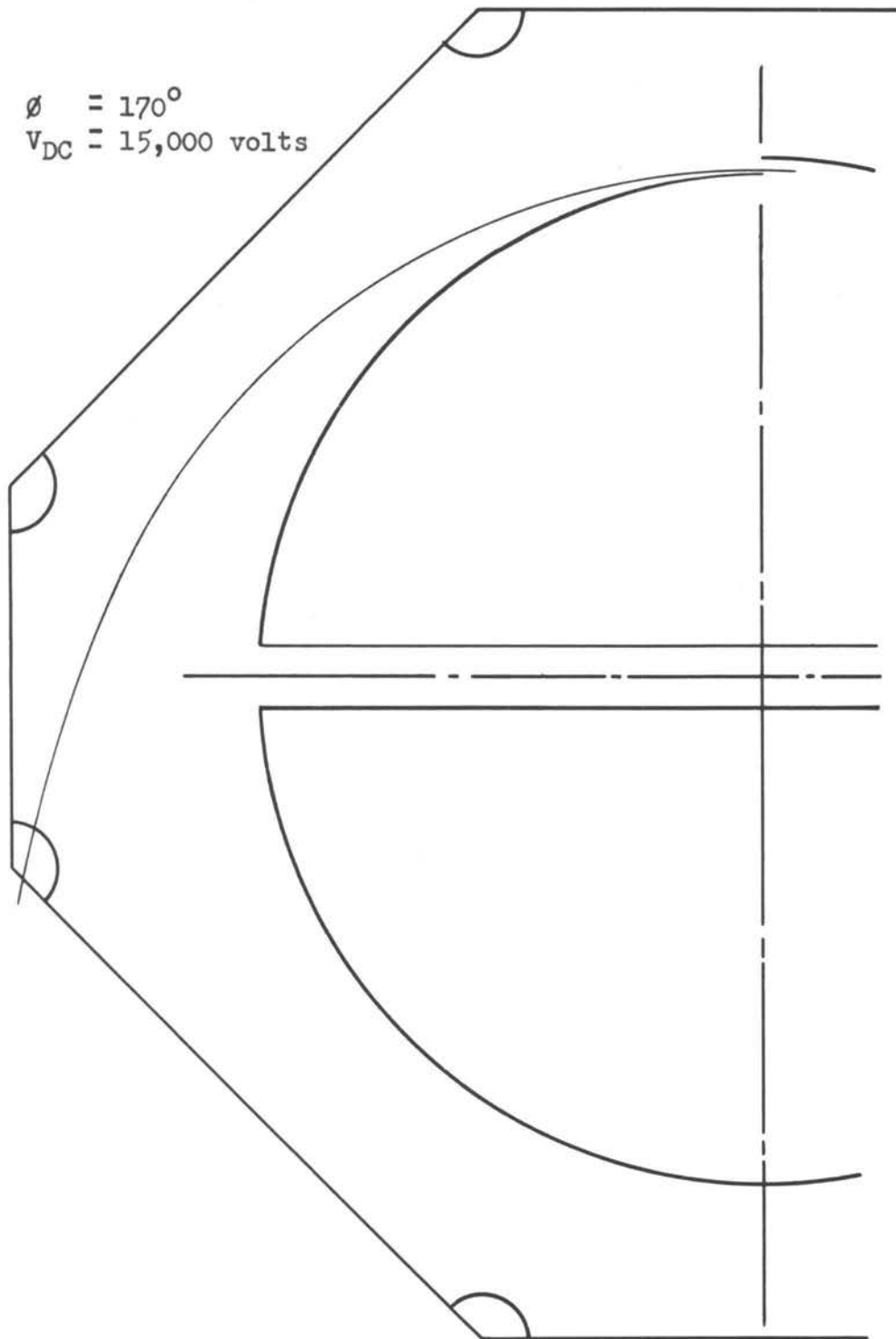


FIGURE 12.
PLOT OF THE ION PATH

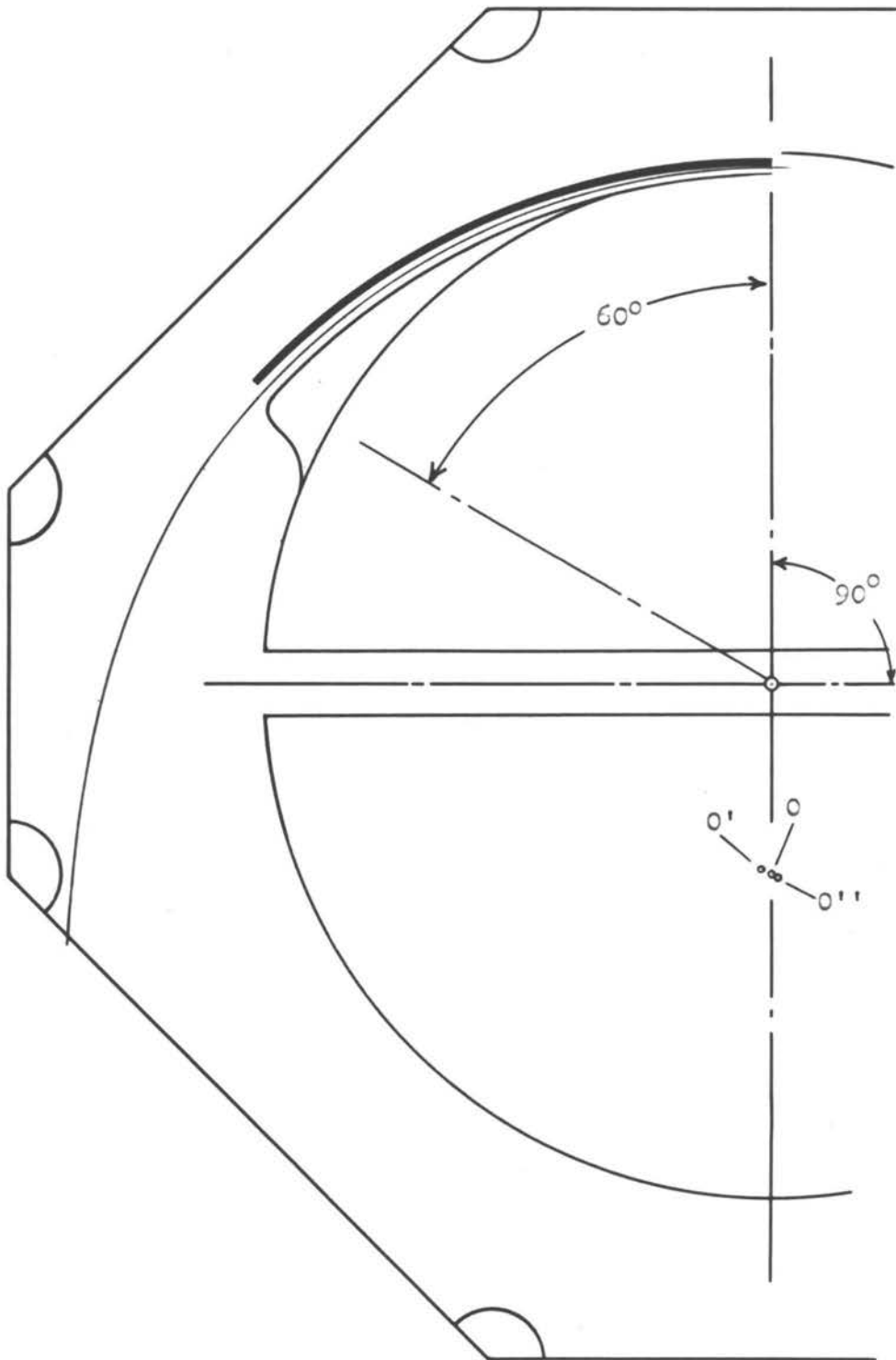


FIGURE 13.

FINAL DEFLECTOR GEOMETRY

CONCLUSION

The results obtained from calculating the path of ions with various phases through a channel beginning at either 80 or 90 degrees past the dee gap with different potentials on the deflector are listed in Table 4. Their respective plots may be found in Figures 8 through 12.

In Figures 10, 11, and 12, the effect of varying the phase, location of the channel entrance and D.C. bias while holding the point of exit from the vacuum chamber comparatively constant may be noted. (The ions whose paths are shown in Figures 10, 11, and 12 have been deflected more than would be required, so that a lesser D.C. bias potential may be applied to the deflector.) In Figures 8, 9, and 10 the effect of varying the bias voltage and location of the channel entrance on the exit of the beam from the vacuum chamber for an ion of constant phase is shown. The deflection produced by the average deflecting field which may be obtained from Table 3 may be checked for each plot. However, it will be noted that the deflecting fields for paths shown in Figures 10, 11, and 12 are essentially the same while there is quite a difference between the fields for the paths in Figures 8, 9, and 10.

Calculations here are necessarily of a preliminary nature preceding measurement of the phase of the ions when the machine is in operation. The magnetic field should be measured to larger radii and the values for lesser radii checked with those previously taken to determine any change, which if observed, may affect the future

operation of the machine. Since the geometry has been determined by making use of certain assumptions, e.g. the energy and direction of the ions at the channel entrance, these should be measured experimentally.

It appears, however, from the information available at this time about the Oregon State College cyclotron and the deflectors already in use for other fixed frequency cyclotrons, that the final deflector geometry may be approximately that shown in Figure 13, with 10,000 volts bias applied to the deflector. While an ion beam as shown in Figure 9 has been brought out from the cyclotron without any bias applied to the deflector, the range obtainable in adjusting the electrostatic field by moving the deflector in and out may not be sufficient to bring the maximum ion beam current possible out to the target. For this reason, a deflector with 10,000 volts D.C. bias applied and a channel starting at 90 degrees past the dee gap has been suggested. (This is assuming that the phase of the mean ion will be about 150 degrees.) The suggested channel entrance and exit widths are 0.21 and 0.42 inch respectively. The average centers of curvature for the ion path, the deflector, and the built out side of the dee, have been located in Figure 13 as O, O' and O'' respectively.

While the problem of deflecting 7.5 Mev deuterons has been discussed, it may easily be extended to the deflection of alpha particles, since they have approximately the same q/m ratio. Protons would be expected to be deflected more in the same field since their q/m ratio is about half that for the deuteron case. However, these

VALUES FOR THE COMPUTATIONS USED IN PLOTTING THE ION PATHS

$\phi = 150^\circ$ $V_{DC} = 10,000$ Volts $\theta = 90^\circ - 150^\circ$

Path
Plotted
in Figures
8 and 13

R_1	θ	R	B(R)	$\frac{B(R)}{B_0}$
inches	degrees	Inches	Gauss	--
21.8	90	16.0	13,870	1.000
27.0	100	16.0	13,870	1.000
21.6	110	16.2	13,820	0.998
21.3	120	16.6	13,660	0.985
20.1	130	17.0	13,440	0.970
21.0	140	17.7	12,850	0.927
21.6	150	18.3	12,120	0.875
20.3	160	19.1	10,900	0.787
24.6	170	20.0	9,000	0.650
30.6	180	20.9	7,250	0.523

$\phi = 150^\circ$ $V_{DC} = 0$ $\theta = 80^\circ - 140^\circ$

Path
Plotted in
Figure 9

R_1	θ	R	B(R)	$\frac{B(R)}{B_0}$
inches	degrees	inches	Gauss	--
19.8	80	16.0	13,870	1.000
20.2	90	16.0	13,870	1.000
20.2	100	16.15	13,800	0.998
20.2	110	16.4	13,660	0.986
19.6	120	16.7	13,610	0.983
19.6	130	17.2	13,300	0.960
19.8	140	17.7	12,850	0.927
18.1	150	18.2	12,260	0.885
20.0	160	18.9	11,100	0.802
21.3	170	19.4	10,400	0.750
26.7	180	20.1	8,300	0.600
36.8	190	21.0	6,000	0.435

Table 4

Path Plotted in Figure 10		$\phi = 150^\circ$ $V_{DC} = 20,000$ Volts $\theta = 90^\circ - 150^\circ$				
		R_1	θ	R	B(R)	$\frac{B(R)}{B_0}$
		inches	degrees	inches	Gauss	--
	23.4	90	16.0	13,870	1.000	
	23.5	100	16.0	13,870	1.000	
	23.1	110	16.3	13,780	0.995	
	23.4	120	16.7	13,610	0.983	
	22.0	130	17.3	13,230	0.955	
	22.3	140	17.9	12,640	0.913	
	21.5	150	18.6	11,720	0.846	
	22.7	160	19.5	9,750	0.705	
	30.4	170	20.5	7,300	0.526	
	49.3	180	21.8	4,500	0.325	

Path Plotted in Figure 11		$\phi = 160^\circ$ $V_{DC} = 10,000$ Volts $\theta = 80^\circ - 140^\circ$				
		R_1	θ	R	B(R)	$\frac{B(R)}{B_0}$
		inches	degrees	inches	Gauss	--
	22.0	80	16.0	13,870	1.000	
	21.8	90	16.1	13,840	0.999	
	20.2	100	16.35	13,760	0.994	
	19.9	110	16.6	13,660	0.985	
	20.6	120	17.0	13,450	0.970	
	20.6	130	17.5	13,060	0.943	
	21.3	140	18.2	12,260	0.885	
	20.0	150	18.9	11,100	0.802	
	24.0	160	19.7	7,100	0.513	
	31.2	170	20.6	4,500	0.315	

Table 4 (Continued)

Path
Plotted in
Figure 12

$\phi = 170^\circ$ $V_{DC} = 15,000$ Volts, $\theta = 90^\circ - 150^\circ$

R_1	θ	R	B(R)	$\frac{B(R)}{B_0}$
inches	degrees	inches	Gauss	--
	90	16.0	13,869	1.000
	100	16.1	13,840	0.999
	110	16.3	13,780	0.995
	120	16.65	13,635	0.984
	130	17.20	13,304	0.960
	140	17.8	12,760	0.920
	150	18.6	11,720	0.846
	160	19.4	10,400	0.750
	170	20.3	7,250	0.523
	180	21.5	5,500	0.396

Table 4 (Continued)

may be deflected with the same geometry, approximately, by some combination of a decreased bias voltage and a wider spacing in the channel. In any case, experiment will be more valuable than theory in determining exactly the final deflection conditions.

BIBLIOGRAPHY

1. Allen, A. J., M. B. Sampson and R. G. Franklin. The cyclotron of the Biochemical research foundation. Journal of the Franklin institute 228:543-561. 1939.
2. Bates, David J. Measurements on the magnetic field of the Oregon state college cyclotron. Master's thesis. Corvallis, Oregon state college, 1953. 83 numb. leaves.
3. Chew, Geoffrey F. and Burton J. Moyer. High energy accelerators at the university of California radiation laboratory. American journal of physics 18:125-136. 1950.
4. Fremlin, J. H. and J. S. Gooden. Cyclic accelerators. Reports on progress in physics 13:295-349. 1950.
5. Gallop, J. W. Notes on a tour of American fixed frequency cyclotrons in the autumn of 1950. London, Medical research council, radiotherapeutic research unit, 1950. 84 p. (Mimeographed).
6. Harlow, Francis H. The cyclotron beam. Seattle, university of Washington, September, 1951. 48 p. (Mimeographed).
7. Henderson, Malcolm C. and Milton G. White. The design and operation of a large cyclotron. Review of scientific instruments 9:19-30. 1938.
8. Henderson, W. J., et al. The Purdue cyclotron. Journal of the Franklin institute 228:563-579. 1939.
9. Hutter, R. G. E. The deflection of beams of charged particles. Advances in electronics 1:167-218. 1948.
10. Kruger, P. Gerald and G. K. Green. The construction and operation of a cyclotron to produce one million volt deuterons. Physical review 51:699-705. 1937.
11. Kruger, P. Gerald, et al. A cyclotron which allows the accelerated particles to emerge in a direction parallel to the dee interface. Review of scientific instruments 15:333-339. 1944.

12. Kurie, Franz N. Present-day design and technique of the cyclotron. *Journal of applied physics* 9:691-701. 1938.
13. Lawrence, Ernest O. and M. Stanley Livingston. The production of high speed light ions without the use of high voltages. *Physical review* 40:19-35. 1932.
14. Lawrence, Ernest O. and M. Stanley Livingston. The multiple acceleration of ions to very high speeds. *Physical review* 45:608-612. 1934.
15. Lawrence, Ernest O. and Donald Cooksey. On the apparatus for the multiple acceleration of light ions to high speeds. *Physical review* 50:1131-1140. 1936.
16. Livingston, M. Stanley. The magnetic resonance accelerator. *Review of scientific instruments* 7:55-68. 1936.
17. Livingston, M. Stanley. The cyclotron. *Journal of applied physics* 15:2-19, 128-147. 1944.
18. Livingston, M. Stanley. Particle accelerators. *Advances in electronics* 1:269-315. 1948.
19. Lofgren, E. J. A high intensity cyclotron. *Physical review* 76:587. 1949.
20. Mann, W. B. The cyclotron and some of its applications. *Reports on progress in physics* 6:125-136. 1939.
21. Mann, W. B. The cyclotron. New York, Chemical publishing company, 1939. 92 p.
22. Murray, Raymond L. and Lawrence T. Ratner. Electric fields within cyclotron dees. *Journal of applied physics* 24:67-69. 1953.
23. Neher, Leland K. Variations in beam current of the 60" cyclotron. 8/23/47. (Photostated Crocker laboratory report, UCRL. 60-52).
24. Neher, Leland K. The r.f. deflector problem for the 60" cyclotron. 9/20/49. (Photostated Crocker laboratory report, UCRL. 60-50).
25. Pickavance, T. G. Cyclotrons. *Progress reports in nuclear physics* 1:1-20. 1950.

26. Rose, M. E. Focusing and maximum energy in the cyclotron. *Physical review* 23:392-408. 1938.
27. Schmidt, F. H. et al. The university of Washington sixty-inch cyclotron. *Review of scientific instruments* 25:499-510. 1954.
28. Thomas, L. H. The paths of ions in the cyclotron. *Physical review* 54:580-598. 1938.
29. Wilson, Robert R. Magnetic and electrostatic focusing in the cyclotron. *Physical review* 53:408-420. 1938.
30. Wilson, Robert R. Theory of the cyclotron. *Journal of applied physics* 11:781-796. 1940.